Organocatalytic reduction

We have examined the catalytic mechanism of an amino acid ester salts in the transfer hydrogenation between the Hantzsch ester and the 3-metil-2-ciklohexen-1-one using the ωB97X-D density functional method. In the literature, two different reaction mechanisms have been proposed, namely the iminium catalysis for the organocatalytic reaction and the hydrogen-bond catalysis for the enzymatic reduction. We compared the two activation modes focusing on the step of the hydride transfer and the results suggest that the iminium pathway is more favorable for the organocatalytic reaction. The effect of the acid cocatalyst was neglected in previous DFT calculations but we found that the conjugate base has an important role in the stabilization of the transition states. Previous theoretical studies showed that the proton and the hydride transfer proceed in two distinct steps in the enzymatic reaction. In contrast with those findings, we observed that the proton and the hydride transfers occur in a concerted fashion for the hydrogen bond mechanism leading to an enol intermediate.

Enzymatic reduction

We have compared two possible mechanisms for the rate determining step of an enzyme catalyzed reduction to determine the most favored reaction path. One of the possibilities is the hydrogen bond activated route, which has been studied in detail by Lonsdale using QM/MM methods in 2015. From the x-ray crystal structure of the enzyme, crystalized with its competitive inhibitor substrates, para substituted phenolic compounds (para-nitrophenol, parahydroxybenzaldehyde) this pathway seems reasonable. Although examining the analogous organocatalytic reaction it turns out that in that case an iminium-ion activated reaction path is favored, that yields an enamine intermediate. With the lysine present in the active center of the enzyme an opportunity arises for the iminium activated mechanism in the biocatalytic case as well. Moreover, in the homologous enzymes this amino acid is always present at the active center. By applying the so called “Quantum chemical cluster” approach, that means, that model systems, including the four most important amino acids in the active center, the substrate and a flavin molecule, have been built which have been treated by ωB97X-D DFT functional, meanwhile the chain ends of the amino acids were frozen in their x-ray structure position. Using the described method several transition states were found for the two possible routes. This method has the advantage that the two pathways can be compared directly in free energies. Based upon the results the iminium activated pathway seems to be the more favored one over the hydrogen bond activated, although the calculations significantly overestimate the experimental barrier heights. The difference between the barrier heights is around 10 kcal/mol in every transition

state. Moreover, it turned out, that lysine might play an important role in the mechanism on the hydrogen bond activated path as well.

Beyond the “Quantum chemical cluster” approach, we also performed several QM/MM calculations using Lonsdale's work as a basis for this enzymatic reduction study, which we were able to reproduce. Unfortunately, when we reviewed Lonsdale's calculations, we found several shortcomings that questions the accuracy of the results. Although we also investigated the iminium pathway, we could not resolve the discrepancies.

Investigation of other catalytic reactions

During the reporting period, we were involved in the study of an organocatalytic Michael reaction and a Mannich reaction. We are also about to publish a study about the activation mechanism of an initiator in olefin metathesis.

Nuclear quantum effects in the calculation of structural and thermodynamic quantities

We created the foundations of a new procedure for the estimation of thermodynamic and structural properties. To estimate the rate of catalytic reactions, activation free entalpies are used. In these, nuclear quantum effects such as zero-point energy have a significant contribution. These estimates are based on the harmonic oscillator model in static calculations. If one wants to take the effect of anharmonicity into account, much more time-consuming and complex methods are needed. In the long term, we want to develop a method that goes beyond harmonic approximation but can be used routinely. The essence of the method is to map the anharmoniciti with Born-Oppenheimer or classical molecular dynamics, and the resulting trajectories are subsequently quantum corrected. The greatest novelty of our approach is that it can also imitate quantum fluctuations of nuclei. We applied our method to different water phases and analyzed dynamic and structural properties such as self-diffusion coefficients or radial density function of nuclei in addition to thermodynamic quantities. Our process provides more accurate results than the two-phase thermodynamics method, which operates on a similar approach, but it is easy to apply and orders of magnitude faster than path integral molecule dynamics simulation. We also tested our method for the heat capacity and self-diffusion coefficients of organic liquids. A manuscript about this study is before submission and appended to this document.

Two Faces of the Two-Phase Thermodynamic Model

Ádám Madarász,*,† Andrea Hamza,† Dávid Ferenc,†,‡ and Imre Bakó†

†*Research Centre for Natural Sciences, Magyar Tudósok Körútja 2, H-1117 Budapest, Hungary*

‡*Institute of Chemistry, ELTE, Eötvös Loránd University, Pázmány Péter sétány 1/A, Budapest, H-1117, Hungary*

Received October 30, 2020; E-mail: madarasz.adam@ttk.hu

Abstract:

The quantum harmonics model and the two-phase thermodynamics method (2PT) are widely used to obtain quantum corrected properties such as isobaric heat capacities or molar entropies. Although, excellent correlation with experiment was achieved for several systems, we present that in many cases these nuclear quantum effects are calculated inaccurately, and the excellent correlations are due to error cancellation. We tested the performance of different quantum corrections on the heat capacities of common organic solvents against experimental data. The accuracy of the computations was also assessed with the determination of the self-diffusion coefficients.

Accounting for nuclear quantum effect is essential to obtain meaningful thermodynamic properties that are comparable to experimental observations.[1] The most typical example is that zero point energies are indispensable in the determination of reaction free energies. Berens proposed to add quantum correction to the classically calculated properties using the harmonic oscillator model.[2] Goddard improved this by the separation of different motions like translation rotations and vibrations and using different functions for each of them.[3,4] This was abbreviated as two-phase thermodynamics (2PT) referring to the gas phase and solid phase motions in contrast to the one-phase thermodynamics (1PT) method where only vibrations were considered. The 1PT method, however is different from what Berens originally proposed, since the latter also included an anharmonic correction, and thus we refer to that method as one-phase-thermodynamics with anharmonic correction (1PT+AC). The 2PT model was validated on Lennard-Jones fluids and water against 1PT but not against 1PT+AC.[3,4] In this study we fill this gap and we compare the 2PT method to the 1PT+AC extensively.

2PT and 1PT+AC methods were successfully applied for the calculation of thermodynamic properties of several systems such as Lennard-Jones fluids,[3,5] water,[2,4,6–14] aqueous solutions,[15,16] molten salts,[17] organic liquids,[18–20] carbon dioxide,[21] urea,[22] ionic liquids,[23–25,25] carbohydrates,[26] cellulose,[27] mixtures[28] and interfaces.[29–34] Lately, 2PT was used for the definition of the Frenkel line.[35–38] Both 1PT/2PT methods are still in continuous development in respect of accuracy and applicability.[39–46]

Recently we have shown that Berens' original idea about the quantum correction on thermodynamic properties can be extended to structural properties if the quantum correction is applied in time domain instead of frequency domain.[47] Our technique, generalized smoothed trajectory analysis (GSTA) gives identical results for thermodynamics properties as 1PT+AC, but much more effectively. Regarding the heat capacity of different states of water GSTA/1PT+AC gave better agreement with the experiment than the 2PT method. Besides our study there was no systematic comparison in the literature to determine which method is more accurate, 2PT or 1PT+AC.

Here we analyse heat capacities to evaluate different types of quantum corrections because it contains large nuclear quantum effect and there are accurate experimental data that can be used for the benchmark of force fields.[6,16,18–20,24,25,27,48–57] In contrast to enthalpy or Gibbs energy, heat capacity is an absolute quantity meaning that there is no need to set the zero point. Additionally, the isobaric heat capacity is a state function, so if we know the c_p as function of T and p, the other state functions can be calculated as well such as the enthalpy and entropy. Previously, quantum corrected thermodynamic properties of organic solvents were investigated in two systematic studies by Pascal, and Caleman.[18,19] For the same solvents they found similar results: the 2PT heat capacities were in good agreements with the experimental data. Both studies showed that OPLS force field gave better results than other general force fields such as GAFF or CHARMM. We recalculated the heat capacities of 92 organic solvents from ref 19 to test further the GSTA, 1PT+AC and 2PT methods.

For the determination of the quantum corrected thermodynamic properties the velocity autocorrelation functions (VACF) are computed from molecular dynamics simulations that can be defined as follows:

$$\mathrm{VACF}(t) = \lim_{\tau\to\infty} \frac{1}{2\tau\langle mv^2\rangle} \int_{-\tau}^{+\tau} mv(t+t')\cdot v(t')\mathrm{d}t' \qquad (1)$$

where m is the mass and v is the velocity as a function of the time (t). The vibrational density of states (VDOS) is the Fourier transform of the autocorrelation function (VACF)

$$\mathrm{VDOS}(\nu) = \mathcal{F}_t\left\{\mathrm{VACF}(t)\right\}(\nu) = 2\int_0^{+\infty} \mathrm{VACF}(t)\cdot\cos(2\pi\nu t)\mathrm{d}t \qquad (2)$$

where ν is the frequency. Since the VACF(t) is a real function, the Fourier cosine transform is applied.

Originally Berens proposed that the quantum corrected density of states can be determined by the multiplication of VDOS with an appropriate weight function w:[2]

$$\mathrm{VDOS}^{\mathrm{q}}(\nu) = \mathrm{VDOS}(\nu)\cdot w(\nu) \qquad (3)$$

In the 1PT method there is no separation of motions, all are considered as vibrations. The weight function for the

heat capacity:[58]

$$w_{\mathrm{vib}}^{c_V}(\nu) = \exp(\beta h\nu)\left(\frac{\beta h\nu}{1-\exp(\beta h\nu)}\right)^2 \quad (4)$$

where $\beta = (k_{\mathrm{B}}T)^{-1}$, k_{B} is the Boltzmann constant, T is the temperature, h is the Planck constant. Thus the isochoric heat capacity can be calculated as

$$c_V^{1\mathrm{PT}} = 2fR\int_0^\infty \mathrm{VDOS}(\nu)\cdot w_{\mathrm{vib}}^{c_V}(\nu)\mathrm{d}\nu \quad (5)$$

where R is the universal gas constant, and $f = 3N$ is the number of degrees of freedom of an N-atomic molecule.

Gaseous motions like translation and rotation are separated from vibrations in the 2PT method. The total VDOS is decomposed into two terms, solid and gaseous components:

$$\mathrm{VDOS}(\nu) = \mathrm{VDOS}_{\mathrm{sol}}(\nu) + \mathrm{VDOS}_{\mathrm{gas}}(\nu) \quad (6)$$

Different weight functions are used for the different motions in the calculation of the thermodynamic properties:

$$c_V^{2\mathrm{PT}} = 2fR\int_0^\infty [\mathrm{VDOS}_{\mathrm{sol}}(\nu)w_{\mathrm{vib}}^{c_V}(\nu) + \mathrm{VDOS}_{\mathrm{gas}}w_{\mathrm{gas}}^{c_V}(\nu)]\,\mathrm{d}\nu \quad (7)$$

The weight function of the gaseous component is 1/2 for the heat capacity.[3,4] One limitation of 2PT is that the molecular topology needs to remain the same, so bond breaking/formation, thus chemical reactions, cannot be modeled, moreover intramolecular rotations cannot be described properly even with 2PT.

In the 1PT+AC method a quantum correction (c^{QC}) is added to the classical isochoric heat capacity (c_V^{cl}):[2]

$$c_V^{1\mathrm{PT+AC}} = c_V^{\mathrm{cl}} + c^{\mathrm{QC}} = fR + c^{\mathrm{AC}} + c^{\mathrm{QC}} = c_V^{1\mathrm{PT}} + c^{\mathrm{AC}} \quad (8)$$

where c^{AC} is the anharmonic correction. From eq 8 it can be seen that the 1PT+AC heat capacity is actually a sum of three terms: the heat capacity of f classic harmonic oscillator plus an anharmonic and a quantum correction.

Jorgensen proposed to correct the classical heat capacity by the estimation of the intramolecular component using the ideal gas value taken from experiments or ab initio calculations.[48,49] If a given force field reproduces the experimental heat capacity of the gas accurately then Jorgensen's approach should give similar value to the 1PT+AC method. Some deviation may occur if the frequencies of the intramolecular vibrations differ in the liquid and gas phases.

The isobaric heat capacity can be determined from the isochoric heat capacity by employing the relation

$$c_p = c_V + \frac{TM\alpha_p^2}{\rho\kappa_T}\ , \quad (9)$$

where α_p denotes the thermal expansion coefficient, M is the relative molar mass, ρ is the density and κ_T is the isothermal compressibility. The isobaric 1PT+AC heat capacity is computed as a sum of the classical isobaric heat capacity and the quantum correction from eq 8:

$$c_p^{1\mathrm{PT+AC}} = c_p^{\mathrm{cl}} + c^{\mathrm{QC}} \quad (10)$$

We performed 10.6 ns long NpT simulations by using the GROMACS simulation software.[59] The settings and inputs were taken from the ref 19 (more details can be found in the Supporting Information). 2PT heat capacities were calculated with the "dos" analysis tool of GROMACS. The classical heat capacity was determined from the fluctuation of enthalpy

$$c_p^{\mathrm{cl}} = \left(\frac{\langle\partial H^2\rangle}{RT^2}\right)_p \quad (11)$$

According to the correspondence principle the quantum calculations should agree with the classical results as the h Planck constant formally approaches zero. The 1PT model gives fR for the heat capacity in the classical limit. Applying the classical weight functions of 1/2 and 1 in eq 7 it is easy to see, that the 2PT model can give values between $fR/2$ and fR for the isochoric heat capacities in the classical limit. The 1PT+AC model always satisfies the correspondence principle in contrast with the 1PT or 2PT methods:

$$\lim_{h\to 0} c_p^{1\mathrm{PT+AC}} = c_p^{\mathrm{cl}} \quad (12)$$

This also implies that the technique is able to describe the effects of anharmonic motions. The 2PT isochoric heat capacities for a rigid water model with 3 translational and 3 rotational degrees of freedom must be below $6R = 49.9$ J/mol/K. The fact that in ref 9, 10, 16, 31 the calculated 2PT heat capacities are in the range of 57 and 81 J/K/mol which is significantly larger than the theoretical limit of 49.9 J/K/mol implies some errors in the computations.

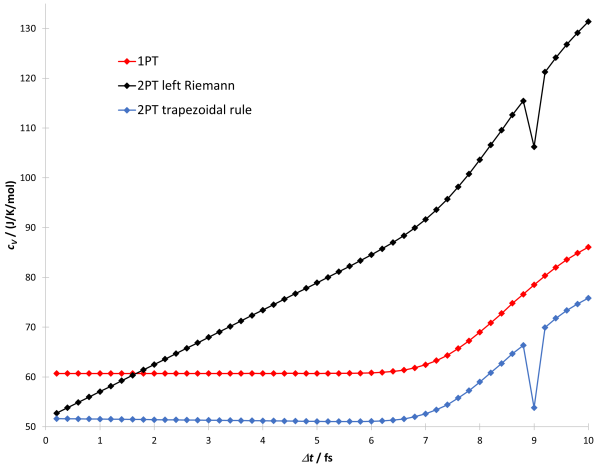

Figure 1. Convergence of the isochoric heat capacity of methanol as a function of step size

In our previous study we showed that the 1PT+AC heat capacity can be significantly overestimated if the left Riemann sum is used instead of the trapezoidal rule in the computation of VDOS in eq 2.[47] To check whether this numerical error can occur in the calculation of the 2PT heat capacities, we tested thoroughly the "dos" analysis tool of the GROMACS that was used in ref 19. The default Fast Fourier Transformation routine in GROMACS applies the left Riemann rule but we also implemented a simple trapezoidal integral rule. On the example of methanol we found, that by decreasing the integration time step the trapezoidal integral converged rapidly at 5 fs, meanwhile the default left Riemann sum gave the correct 2PT heat capacity, 51.6 J/K/mol only in the $\Delta t \to 0$ limit (see Figure 1). At 4 fs time step, which is generally used in 2PT calculations, the heat capacity of 73.4 J/K/mol is overestimated by 40 %. This agrees well with the result of 75.8 J/K/mol from ref 19. The convergence of the 1PT method is also shown with the trapezoidal formula, and at 4 fs the 1PT heat capacity

is also converged with 60.7 J/K/mol.

When we recalculated the heat capacities of 9 common solvents from ref 18 and 19 with both integral formulas, we reproduced the literature data but we obtained 45 % lower heat capacities with the correct integral formula (see the Supporting Information). In ref 18 and 19 the 2PT heat capacities are similar to each other for the same solvents with OPLS force field, which implies that in both works the same (incorrect) integration routine was used.

Surprisingly, in these previous works excellent correlations were found between the 2PT and experimental isobaric heat capacities. How is it possible that such a good correlation has been achieved, if the values were overestimated with 45 %? It seems that there was an (un)fortunate error cancellation, where the opposite error is connected to the conversion between the isobaric and isochoric heat capacities in eq 9. For stable systems the isobaric heat capacity is always larger than the isochoric heat capacity. The isobaric heat capacities can be measured readily, but isochoric heat capacities are less available in experiments, it can be determined from other properties according to eq 9. In calculations, however, NVT simulations are more widespread than NpT. The latter one needs longer equilibration time, therefore the calculation of isochoric heat capacity is easier.

In ref 19 the c_p c_V difference is always smaller than 0.1 J/K/mol, and in ref 18 this correction was not larger than 1.2 J/K/mol. This is similar to that of liquid water: at 25 °C the difference is only 0.8 J/K/mol between the isobaric and isochoric heat capacities, and their ratio is 1.01.[60] We recalculated the c_p c_V differences for organic liquids from ref 19 and we obtained orders of magnitude higher values. In our computations the average difference is 38.4 J/K/mol, and the heat capacity ratio is 1.31. For a few molecules there are direct experimental data for the isochoric heat capacities (see the Supporting Information). For instance for the methanol and ethanol the $c_p - c_V$ are 14 and 11 J/K/mol, respectively.[61,62] This validates that we calculated correctly the $c_p - c_V$ values.

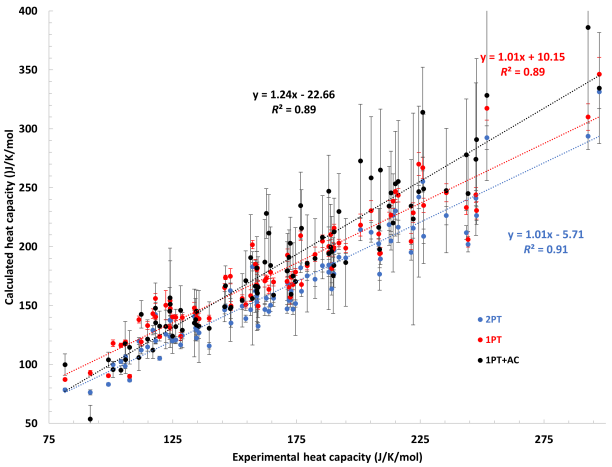

Figure 2. Calculated vs. experimental isobaric heat capacities

The calculated vs. experimental isobaric heat capacities are shown in Figure 2. The overall correlations are good for the predicted and experimental heat capacities, the R^2 is about 0.9 for all three methods. From the fitted lines it can be seen that the slope of the 1PT and 2PT are almost perfect 1.01, but for 1PT+AC the slope is 1.24. The 2PT systematically underestimates, the 1PT overestimates the isobaric heat capacities.

The mean absolute deviations for different types of molecules are shown in Figure 3. For all the compounds the error is 20 J/K/mol for the 1PT+AC method. The error is smaller with 1PT and even smaller with the 2PT method. The methods perform differently for different types of compounds, and even their relative goodness is varying. For hydrocarbons, organosulfures, halocarbons and heteroaromatics the 1PT performs the worst, and the 1PT+AC and 2PT performs similarly better. For amines, ethers, alcohols and ketones the 1PT+AC performs the worst, and the 1PT and 2PT methods perform much better. The large errors of the 1PT+AC heat capacities may originate from the deficiency of the force field and/or from the inaccuracy of the 1PT+AC method. To separate these two errors, we investigated the classical limits which characterize the failure of the method.

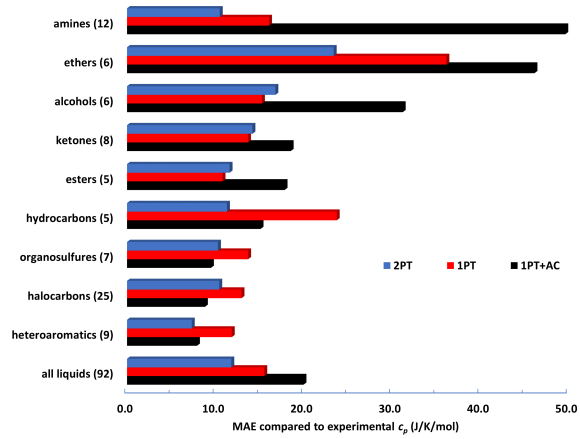

Figure 3. Mean absolute errors (MAE) of the calculated isobaric heat capacities compared to experimental data.

As mentioned above the 1PT and 2PT models do not satisfy the correspondence principle, they cannot reproduce the classical heat capacities of anharmonic cases. To quantify these deviations the mean error of the reproduction of the classical heat capacities is shown for the 1PT and 2PT methods in Figure 4. 1PT+AC is not shown because this error is zero according to eq 12. 2PT always underestimates the classical heat capacity, by 21.4 J/mol/K in average which is almost twice as large as the mean absolute error compared to the experiments, 11.8 J/mol/K. The 1PT method overestimates the classical heat capacity for the heteroaromatics, halocarbons, organosulfures and hydrocarbons and underestimates for the other compound groups. This classification correlates perfectly with the relative performance of 1PT and 1PT+AC in Figure 3. If the 1PT heat capacity agrees better with the experiment than the 1PT+AC, then it means that the anharmonicity is described incorrectly by the force field. The uncertainty of the anharmonicity is too large with the OPLS force field for the aliphatic N and O compounds and this is why the 2PT method estimates the heat capacity of organic liquids more accurately. These results suggest that the effect of anharmonicity is significantly smaller than the quantum effect on the heat capacity of the organic liquids. In the 1PT+AC method this means that the size of the anharmonic correction is smaller than that of the quantum correction in eq 8.

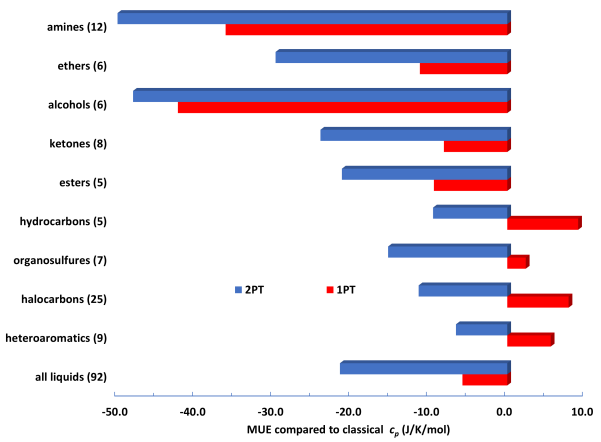

Figure 4. Mean unsigned errors (MUE) of the isobaric heat capacities in the classical limit.

Caleman and Pascal concluded from their studies that the reproduction of the experimental heat capacities could be improved by better description of the the force constants of bonds and angles.[18,19] This is true for the quantum correction, but the anharmonic correction can be adjusted with the non-bonding parameters. Our results suggest that the thermodynamics properties are more sensitive to the intermolecular interactions than to the intramolecular interactions. This is in line with the general experiences that in the simulation of the organic liquids the bond lengths and angles can be constrained at room temperature.

To estimate the consistency of the calculations of VACF and VDOS functions we computed the self-diffusion coefficients with two different methods.[63] First, we determined D_s from the VACF:

$$D_{\mathrm{s}} = \frac{\langle v^2 \rangle}{3} \lim_{t\to\infty} \int_0^t \mathrm{VACF}(\tau)\mathrm{d}\tau \qquad (13)$$

The self-diffusion coefficient can also be calculated from the mean square displacement of the atoms using the Einstein equation:

$$D_{\mathrm{s}} = \lim_{t\to\infty} \frac{\partial \langle (x(t) - x(0))^2 \rangle}{6\partial t} \qquad (14)$$

We computed the self-diffusion coefficients according to these equations at 10 ps. The two complementary approaches gave almost identical results (MAE $= 0.05 \cdot 10^{-9}\mathrm{m}^2\mathrm{s}^{-1}$, $R^2 = 0.998$) which validates how we calculated the VACF and VDOS functions (see the Supplementary Information). The self-diffusion coefficients were also determined from the 10 ns simulations using eq 14. Comparing to the available experimental data the mean absolute error is $0.62 \cdot 10^{-9}\mathrm{m}^2\mathrm{s}^{-1}$ for 31 liquids, which means significant correlation ($R^2 = 0.79$) (see Figure 5). It looks that the values have not converged at 10 ps but the longer simulation time (10 ns vs. 10 ps) does not improve the accuracy of the estimation of the self-diffusion coefficient. Actually, the mean absolute error is slightly lower, $0.55 \cdot 10^{-9}\mathrm{m}^2\mathrm{s}^{-1}$ using 10 ps long VACF functions, and the correlation coefficient is almost the same ($R^2 = 0.77$). As far as we know this is the largest data set of 31 organic solvents for experimental benchmark for self-diffusion coefficients, and there are first principal estimations for further 82 liquids. In a previous study 17 organic solvents were investigated and 9 were compared to experiments.[64]

Although, the heat capacity can be calculated from a 50 fs long VACF,[47] the VDOS function converges much slower. The self-diffusion coefficient and the VDOS(0) converges after 100 ps. Nevertheless, MSD values taken from long simulations can be considered as exact values, they did not reproduce the experiments better than the self-diffusion coefficients calculated from the VACF or VDOS of short MD simulations.

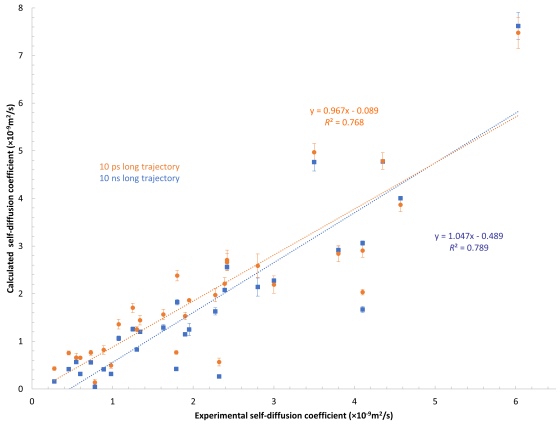

Figure 5. Calculated vs. experimental self-diffusion coefficients in unit of $10^{-9}\mathrm{m}^2\mathrm{s}^{-1}$ for 31 organic solvents

As a summary, we showed that many of the 2PT heat capacities in the literature were calculated incorrectly.[9,10,16,18,19,29,31] The right program code is given in the Supporting Information to calculate the correct 2PT and 1PT thus the more exact 1PT+AC methods by using the GROMACS software. Based on our benchmark calculations we suggest to use different methods for different purposes. Despite of the theoretical limitation of the 2PT method, it can give reasonable estimate for thermodynamic properties of organic liquids using the OPLS force field despite it overestimates anharmonicity of oxygen and nitrogen containing compounds. If someone wants to benchmark force fields, or develop new force field parameters it is advised to use the 1PT+AC method which accounts the anharmonicity correctly. We also showed that our calculation are consistent with the self-diffusion coefficients that was also compared to experimental data. Overall, we found strong correlation ($R^2 = 0.9$) for heat capacities and somewhat moderate correlation ($R^2 = 0.79$) for the self-diffusion coefficients.

Acknowledgement This work was supported by the National Research, Development and Innovation Office of Hungary (NKFI, Grant No. K-108721 and PD-121070). A.M. acknowledges the János Bolyai Scholarship from Hungarian Academy of Sciences.

Supporting Information Available

The details of the simulations and the results are available in the Supporting Information.

References

(1) Collinge, G.; Yuk, S. F.; Nguyen, M.-T.; Lee, M.-S.; Glezakou, V.-A.; Rousseau, R. Effect of Collective Dynamics and Anharmonicity on Entropy in Heterogenous Catalysis: Building the Case for Advanced Molecular Simulations. ACS Catal. **2020**, 10, 9236–9260.

(2) Berens, P. H.; Mackay, D. H. J.; White, G. M.; Wilson, K. R. Thermodynamics and quantum corrections from molecular dynamics for liquid water. J. Chem. Phys. **1983**, 79, 2375–2389.
(3) Lin, S.-T.; Blanco, M.; Goddard, W. A. The two-phase model for calculating thermodynamic properties of liquids from molecular dynamics: Validation for the phase diagram of Lennard-Jones fluids. J. Chem. Phys. **2003**, 119, 11792–11805.
(4) Lin, S.-T.; Maiti, P. K.; Goddard, W. A. Two-Phase Thermodynamic Model for Efficient and Accurate Absolute Entropy of Water from Molecular Dynamics Simulations. J. Phys. Chem. B **2010**, 114, 8191–8198.
(5) Chari, S. S. N.; Dasgupta, C.; Maiti, P. K. Scalar activity induced phase separation and liquid–solid transition in a Lennard-Jones system. Soft Matter **2019**, 15, 7275–7285.
(6) Laury, M. L.; Wang, L.-P.; Pande, V. S.; Head-Gordon, T.; Ponder, J. W. Revised Parameters for the AMOEBA Polarizable Atomic Multipole Water Model. J. Phys. Chem. B **2015**, 119, 9423–9437.
(7) Levitt, M.; Hirshberg, M.; Sharon, R.; Laidig, K. E.; Daggett, V. Calibration and Testing of a Water Model for Simulation of the Molecular Dynamics of Proteins and Nucleic Acids in Solution. J. Phys. Chem. B **1997**, 101, 5051–5061.
(8) Waheed, Q.; Edholm, O. Quantum Corrections to Classical Molecular Dynamics Simulations of Water and Ice. J. Chem. Theory Comput. **2011**, 7, 2903–2909.
(9) Yeh, K.-Y.; Huang, S.-N.; Chen, L.-J.; Lin, S.-T. Diffusive and quantum effects of water properties in different states of matter. J. Chem. Phys. **2014**, 141, 044502.
(10) Pascal, T. A.; Schärf, D.; Jung, Y.; Kühne, T. D. On the absolute thermodynamics of water from computer simulations: A comparison of first-principles molecular dynamics, reactive and empirical force fields. J. Chem. Phys. **2012**, 137, 244507.
(11) Millot, M.; Hamel, S.; Rygg, J. R.; Celliers, P. M.; Collins, G. W.; Coppari, F.; Fratanduono, D. E.; Jeanloz, R.; Swift, D. C.; Eggert, J. H. Experimental evidence for superionic water ice using shock compression. Nature Physics **2018**, 14, 297–302.
(12) Naserifar, S.; Goddard, W. A. The quantum mechanics-based polarizable force field for water simulations. J. Chem. Phys. **2018**, 149, 174502.
(13) Naserifar, S.; Goddard, W. A. Anomalies in Supercooled Water at 230 K Arise from a 1D Polymer to 2D Network Topological Transformation. J. Phys. Chem. Lett. **2019**, 10, 6267–6273, PMID: 31560560.
(14) Naserifar, S.; Oppenheim, J. J.; Yang, H.; Zhou, T.; Zybin, S.; Rizk, M.; Goddard, W. A. Accurate non-bonded potentials based on periodic quantum mechanics calculations for use in molecular simulations of materials and systems. J. Chem. Phys. **2019**, 151, 154111.
(15) Caro, M. A.; Lopez-Acevedo, O.; Laurila, T. Redox Potentials from Ab Initio Molecular Dynamics and Explicit Entropy Calculations: Application to Transition Metals in Aqueous Solution. J. Chem. Theory Comput. **2017**, 13, 3432–3441, PMID: 28715635.
(16) Overduin, S. D.; Patey, G. N. Comparison of simulation and experimental results for a model aqueous tert-butanol solution. J. Chem. Phys. **2017**, 147, 024503.
(17) Engelmann, S.; Hentschke, R. Specific heat capacity enhancement studied in silica doped potassium nitrate via molecular dynamics simulation. Scientific Reports **2019**, 9, 7606.
(18) Pascal, T. A.; Lin, S.-T.; Goddard III, W. A. Thermodynamics of liquids: standard molar entropies and heat capacities of common solvents from 2PT molecular dynamics. Phys. Chem. Chem. Phys. **2011**, 13, 169–181.
(19) Caleman, C.; van Maaren, P. J.; Hong, M.; Hub, J. S.; Costa, L. T.; van der Spoel, D. Force Field Benchmark of Organic Liquids: Density, Enthalpy of Vaporization, Heat Capacities, Surface Tension, Isothermal Compressibility, Volumetric Expansion Coefficient, and Dielectric Constant. J. Chem. Theory Comput. **2012**, 8, 61–74.
(20) Greff da Silveira, L.; Jacobs, M.; Prampolini, G.; Livotto, P. R.; Cacelli, I. Development and Validation of Quantum Mechanically Derived Force-Fields: Thermodynamic, Structural, and Vibrational Properties of Aromatic Heterocycles. J. Chem. Theory Comput. **2018**, 14, 4884–4900, PMID: 30040902.
(21) Huang, S.-N.; Pascal, T. A.; Goddard, W. A.; Maiti, P. K.; Lin, S.-T. Absolute Entropy and Energy of Carbon Dioxide Using the Two-Phase Thermodynamic Model. J. Chem. Theory Comput. **2011**, 7, 1893–1901.
(22) Chen, P.; Nishiyama, Y.; Wohlert, J.; Lu, A.; Mazeau, K.; Ismail, A. E. Translational Entropy and Dispersion Energy Jointly Drive the Adsorption of Urea to Cellulose. J. Phys. Chem. B **2017**, 121, 2244–2251.
(23) Chen, M.; Pendrill, R.; Widmalm, G.; Brady, J. W.; Wohlert, J. Molecular Dynamics Simulations of the Ionic Liquid 1-n-Butyl-3-Methylimidazolium Chloride and Its Binary Mixtures with Ethanol. J. Chem. Theory Comput. **2014**, 10, 4465–4479.
(24) Doherty, B.; Zhong, X.; Gathiaka, S.; Li, B.; Acevedo, O. Revisiting OPLS Force Field Parameters for Ionic Liquid Simulations. J. Chem. Theory Comput. **2017**, 13, 6131–6145.
(25) Doherty, B.; Zhong, X.; Acevedo, O. Virtual Site OPLS Force Field for Imidazolium-Based Ionic Liquids. J. Phys. Chem. B **2018**, 122, 2962–2974, PMID: 29473749.
(26) Wohlert, J. Vapor Pressures and Heats of Sublimation of Crystalline β-Cellobiose from Classical Molecular Dynamics Simulations with Quantum Mechanical Corrections. J. Phys. Chem. B **2014**, 118, 5365–5373.
(27) Bregado, J. L.; Tavares, F. W.; Secchi, A. R.; Segtovich, I. S. V. Thermophysical Properties of Amorphous-Paracrystalline Celluloses by Molecular Dynamics. Macromol. Theory Simul. **2020**, 29, 2000007.
(28) Lai, P.-K.; Hsieh, C.-M.; Lin, S.-T. Rapid determination of entropy and free energy of mixtures from molecular dynamics simulations with the two-phase thermodynamic model. Phys. Chem. Chem. Phys. **2012**, 14, 15206–15213.
(29) Pascal, T. A.; Goddard, W. A. Interfacial Thermodynamics of Water and Six Other Liquid Solvents. J. Phys. Chem. B **2014**, 118, 5943–5956.
(30) Varanasi, S. R.; Subramanian, Y.; Bhatia, S. K. High Interfacial Barriers at Narrow Carbon Nanotube–Water Interfaces. Langmuir **2018**, 34, 8099–8111, PMID: 29905485.
(31) Shrestha, B. R.; Pillai, S.; Santana, A.; Donaldson Jr., S. H.; Pascal, T. A.; Mishra, H. Nuclear Quantum Effects in Hydrophobic Nanoconfinement. The Journal of Physical Chemistry Letters **2019**, 10, 5530–5535, PMID: 31365261.
(32) Mukherjee, S.; Bagchi, B. Entropic Origin of the Attenuated Width of the Ice–Water Interface. J. Phys. Chem. C **2020**, 124, 7334–7340.
(33) Merinov, B. V.; Naserifar, S.; Zybin, S. V.; Morozov, S.; Goddard, W. A.; Lee, J.; Lee, J. H.; Han, H. E.; Choi, Y. C.; Kim, S. H. Li-diffusion at the interface between Li-metal and [Pyr14][TFSI]-ionic liquid: Ab initio molecular dynamics simulations. J. Chem. Phys. **2020**, 152, 031101.
(34) Rokoni, A.; Sun, Y. Probing the temperature profile across a liquid–vapor interface upon phase change. J. Chem. Phys. **2020**, 153, 144706.
(35) Yoon, T. J.; Ha, M. Y.; Lee, W. B.; Lee, Y.-W. "Two-Phase" Thermodynamics of the Frenkel Line. J. Phys. Chem. Lett. **2018**, 9, 4550–4554, PMID: 30052454.
(36) Yoon, T. J.; Ha, M. Y.; Lazar, E. A.; Lee, W. B.; Lee, Y.-W. Topological Characterization of Rigid–Nonrigid Transition across the Frenkel Line. J. Phys. Chem. Lett. **2018**, 9, 6524–6528.
(37) Yoon, T. J.; Patel, L. A.; Ju, T.; Vigil, M. J.; Findikoglu, A. T.; Currier, R. P.; Maerzke, K. A. Thermodynamics, dynamics, and structure of supercritical water at extreme conditions. Phys. Chem. Chem. Phys. **2020**, 22, 16051–16062.
(38) Ghosh, K.; Krishnamurthy, C. V. Frenkel line crossover of confined supercritical fluids. Sci. Rep. **2019**, 9, 14872.
(39) Desjarlais, M. P. First-principles calculation of entropy for liquid metals. Phys. Rev. E **2013**, 88, 062145.
(40) Caro, M. A.; Laurila, T.; Lopez-Acevedo, O. Accurate schemes for calculation of thermodynamic properties of liquid mixtures from molecular dynamics simulations. J. Chem. Phys. **2016**, 145, 244504.
(41) Sun, T.; Xian, J.; Zhang, H.; Zhang, Z.; Zhang, Y. Two-phase thermodynamic model for computing entropies of liquids reanalyzed. J. Chem. Phys. **2017**, 147, 194505.
(42) Persson, R. A. X.; Pattni, V.; Singh, A.; Kast, S. M.; Heyden, M. Signatures of Solvation Thermodynamics in Spectra of Intermolecular Vibrations. J. Chem. Theory Comput. **2017**, 13, 4467–4481.
(43) Pannir Sivajothi, S. S.; Lin, S.-T.; Maiti, P. K. Efficient Computation of Entropy and Other Thermodynamic Properties for Two-Dimensional Systems Using Two-Phase Thermodynamic Model. J. Phys. Chem. B **2019**, 123, 180–193.
(44) Dietschreit, J. C. B.; Peters, L. D. M.; Kussmann, J.; Ochsenfeld, C. Identifying Free Energy Hot-Spots in Molecular Transformations. J. Phys. Chem. A **2019**, 123, 2163–2170.
(45) Li, S.; Pokuri, B. S. S.; Ryno, S. M.; Nkansah, A.; De'Vine, C.; Ganapathysubramanian, B.; Risko, C. Determination of the Free Energies of Mixing of Organic Solutions through a Combined Molecular Dynamics and Bayesian Statistics Approach. J. Chem. Inf. Model **2020**, 60, 1424–1431, PMID: 31935097.
(46) Bernhardt, M. P.; Dallavalle, M.; der Vegt, N. F. A. V. Application of the 2PT model to understanding entropy change in molecular coarse-graining. Soft Materials **2020**, 0, 1–16.
(47) Berta, D.; Ferenc, D.; Bakó, I.; Madarász, A. Nuclear Quantum Effects from the Analysis of Smoothed Trajectories: Pilot Study for Water. J. Chem. Theory Comput. **2020**, 16, 3316–3334, PMID: 32268067.
(48) Jorgensen, W. L. Optimized intermolecular potential functions for liquid alcohols. J. Phys. Chem. **1986**, 90, 1276–1284.
(49) Jorgensen, W. L.; Maxwell, D. S.; Tirado-Rives, J. Development and Testing of the OPLS All-Atom Force Field on Conformational Energetics and Properties of Organic Liquids. J. Am. Chem. Soc. **1996**, 118, 11225–11236.
(50) Cadena, C.; Zhao, Q.; Snurr, R. Q.; Maginn, E. J. Molecular Modeling and Experimental Studies of the Thermodynamic and Transport Properties of Pyridinium-Based Ionic Liquids. J. Phys. Chem. B **2006**, 110, 2821–2832, PMID: 16471891.
(51) Lagache, M.; Ungerer, P.; Boutin, A.; Fuchs, A. H. Prediction of thermodynamic derivative properties of fluids by Monte Carlo simulation. Phys. Chem. Chem. Phys. **2001**, 3, 4333–4339.
(52) Lagache, M.; Ungerer, P.; Boutin, A. Prediction of thermodynamic derivative properties of natural condensate gases at high pressure by Monte Carlo simulation. Fluid Ph. Equilibria **2004**, 220, 211 – 223.

(53) Ungerer, P.; Collell, J.; Yiannourakou, M. Molecular Modeling of the Volumetric and Thermodynamic Properties of Kerogen: Influence of Organic Type and Maturity. Energy & Fuels **2015**, 29, 91–105.
(54) Gong, Z.; Sun, H.; Eichinger, B. E. Temperature Transferability of Force Field Parameters for Dispersion Interactions. J. Chem. Theory Comput. **2018**, 14, 3595–3602, PMID: 29800527.
(55) Smith, W. R.; Jirsák, J.; Nezbeda, I.; Qi, W. Molecular simulation of caloric properties of fluids modelled by force fields with intramolecular contributions: Application to heat capacities. J. Chem. Phys. **2017**, 147, 034508.
(56) Tenney, C. M.; Massel, M.; Mayes, J. M.; Sen, M.; Brennecke, J. F.; Maginn, E. J. A Computational and Experimental Study of the Heat Transfer Properties of Nine Different Ionic Liquids. J. Chem. Eng. Data **2014**, 59, 391–399.
(57) Doherty, B.; Acevedo, O. OPLS Force Field for Choline Chloride-Based Deep Eutectic Solvents. The Journal of Physical Chemistry B **2018**, 122, 9982–9993, PMID: 30125108.
(58) McQuarrie, D.; Simon, J. Molecular Thermodynamics; University Science Books, 1999.
(59) Abraham, M. J.; Murtola, T.; Schulz, R.; Páll, S.; Smith, J. C.; Hess, B.; Lindahl, E. GROMACS: High performance molecular simulations through multi-level parallelism from laptops to supercomputers. SoftwareX **2015**, 1-2, 19 – 25.
(60) Engineering ToolBox, Water - Specific Heat. 2004; `https://www.engineeringtoolbox.com/specific-heat-capacity-water-d_660.html`, accessed September 2020.
(61) Engineering ToolBox, Methanol - Specific Heat. 2018; `https://www.engineeringtoolbox.com/methanol-CH3OH-specific-heat-capacity-Cp-Cv-isobaric-isochoric-d_2103.html`, accessed September 2020.
(62) Engineering ToolBox, Ethanol - Specific Heat. 2018; `https://www.engineeringtoolbox.com/specific-heat-capacity-ethanol-Cp-Cv-isobaric-isochoric-ethyl-alcohol-d_2030.html`, accessed September 2020.
(63) Frenkel, D.; Smit, B. Understanding Molecular Simulation: From Algorithms to Applications, 2nd ed.; Computational Science Series; Academic Press: San Diego, 2002; Vol. 1.
(64) Wang, J.; Hou, T. Application of molecular dynamics simulations in molecular property prediction II: Diffusion coefficient. J. Comput. Chem. **2011**, 32, 3505–3519.

Graphical TOC Entry